Journal of Magnetism and Magnetic Materials 390 (2015) 50–55

Contents lists available at ScienceDirect

Journal of Magnetism and Magnetic Materials

journal homepage: www.elsevier.com/locate/jmmm

Mössbauer spectroscopic analysis and temperature dependent electrical study of $Mg_{0.9}Mn_{0.1}Gd_yFe_{2-y}O_4$ nanoferrites

Gagan Kumar [a,*], Jyoti Shah [b], R.K. Kotnala [b], Virender Pratap Singh [a], Meenakshi Dhiman [c], Sagar E. Shirsath [d], M. Shahbuddin [e], Khalid M. Batoo [f], M. Singh [a]

[a] Department of Physics, Himachal Pradesh University, Shimla 171005, India
[b] CSIR-National Physical Laboratory, Dr. K. S. Krishnan Road, New Delhi 110012, India
[c] Department of Physics, IEC University, Atal Nagar, Kallujhanda, Baddi, India
[d] Spin Device Technology Center, Faculty of Engineering, Shinshu University, Nagano, Japan
[e] Department of Physics, King Saud University, Riyadh, Saudi Arabia
[f] King Abdullah Institute for Nanotechnology, King Saud University, Riyadh, Saudi Arabia

ARTICLE INFO

Article history:
Received 2 February 2015
Received in revised form
22 April 2015
Accepted 23 April 2015
Available online 24 April 2015

Keywords:
Nanostructures
Electric
Dielectric and magnetic properties

ABSTRACT

Mg–Gd–Mn nanoferrites with formulae $Mg_{0.9}Mn_{0.1}Gd_yFe_{2-y}O_4$, where $y=0.05$, 0.1, 0.2 and 0.3, have been synthesized by solution combustion technique. The dc resistivity was observed to decrease with the increase in temperature. Dielectric constant (ε') and loss tangent ($\tan\delta$) have been found to be increasing with an increase in temperature while with an increase in frequency both have been found to be decreasing. The ac electrical conductivity (σ_{ac}) has been studied as a function of temperature at different frequencies and has been observed to be increasing with the increase in temperature. The Mössbauer spectroscopy has been carried out so as to authenticate our previously reported results on the super-exchange interactions.

1. Introduction

Ferrites are the ferromagnetic materials containing iron (III) oxide as their principal component. Ferrites are technologically important class of magnetic oxides due to their good magnetic properties, high electric resistivity, low eddy current loss and low dielectric loss [1]. The electric, dielectric and magnetic properties of ferrites can be tailored either by changing the microstructure or by incorporation of different metal ions [2,3]. Now-a-days, exploration of the nanosized ferrites is one of the most imperative and rapid growing area of research in the field of nanotechnology [4] to cope with the increased technological demand.

Mg–Mn ferrites are well known technological materials finding applications in various electrical and magnetic devices. The importance of Mg–Mn ferrites lies in their magnetic properties and low electrical conductivity which allow electromagnetic waves to propagate in the medium and make them suitable for applications in microwave devices. Mg–Mn ferrites are widely used in the construction of non-reciprocal devices at microwave frequencies such as circulators, gyrators and phase shifter. In addition to this, they are widely used in computer memory chips, magnetic recording media, and fabrication of radio frequency coils, transformers cores and rod antennas [5–7]. Due to the technological importance of Mg–Mn ferrites many researchers have investigated substituted Mg–Mn ferrites. Singh [8] has synthesized $Mg_xMn_{1-x}Fe_2O_4$ ferrites by conventional ceramic technique and the hot-pressed ceramic technique and then made a comparative study of electric and magnetic properties. Lakshman et al. [9] have synthesized the substituted Mg–Mn ferrites and reported the electric, dielectric and magnetic properties. Kumar et al. [10] have reported the effect of swift heavy ion irradiations on the magnetic properties of Mg–Mn ferrites. Okasha [11] reported the influence of gamma-irradiation on the structural and magnetic properties of Mg–Mn ferrites. Tsay et al. [12] have reported the effect of sintering temperature on the microstructural, magnetic and microwave properties of magnesium-manganese ferrites. Modi et al. [13] have reported the structural properties of co-precipitation synthesized Mg–Mn nanoferrites. Pathak et al. [14] have reported the study of Mg–Mn nanoferrites synthesized via co-precipitation method.

Although, there are reports on the dielectric and magnetic properties of mixed Mg–Mn ferrites but rarely any work has been reported on the Mössbauer and temperature dependent electrical properties of gadolinium substituted Mg–Mn nanoferrites prepared by solution combustion method. Therefore, in this paper, a maiden attempt has been made to investigate the temperature

* Corresponding author. Fax: +91 01792 266097.
E-mail address: bhargava_phy_hpu@yahoo.co.in (G. Kumar).

http://dx.doi.org/10.1016/j.jmmm.2015.04.096
0304-8853/

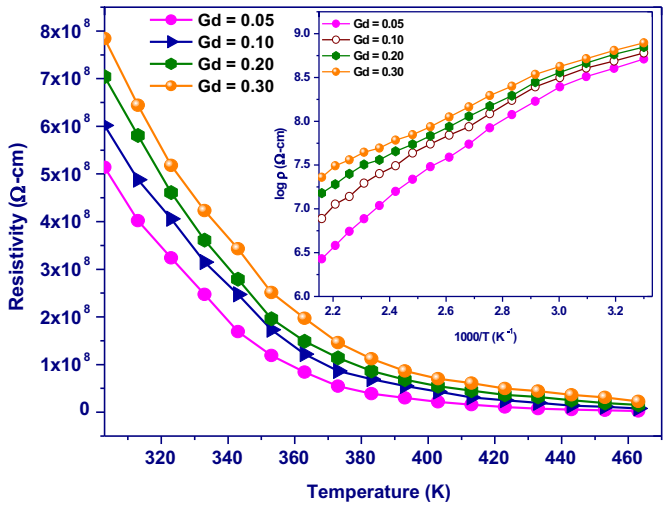

Fig. 1. Variation of dc resistivity with temperature for $Mg_{0.9}Mn_{0.1}Gd_yFe_{2-y}O_4$ nanoferrites.

Table 1
Variations of activation energy for $Mg_{0.9}Mn_{0.1}Gd_yFe_{2-y}O_4$ nanoferrites.

Composition (y)	Activation energy (eV)		
	E_f	E_p	ΔE
0.05	1.22	1.45	0.23
0.1	1.38	1.72	0.34
0.2	1.44	2.25	0.81
0.3	1.69	2.67	0.98

dependent electric, dielectric and ac conductivity behavior of Gd^{3+} substituted Mg–Mn nanoferrites synthesized by solution combustion method.

In past some researchers have reported the weakening of super-exchange interactions with the substitution of gadolinium content [15–18], and many have claimed the increasing trend in the super-exchange interactions with the increasing content of Gd^{3+} ions [19,20]. Therefore, due to above mentioned results for Gd^{3+} substitution we aimed to understand the effect of Gd^{3+} ions on the exchange interactions in details. Recently, we had reported the detailed theoretical discussions along with experimental results regarding the effects on the super-exchange interactions with the substitution of Gd^{3+} ions in the Mg–Mn nanoferrite matrix [21]. Since, the Mössbauer spectroscopy is one of the important techniques which can measure the comparatively weak interactions between the nucleus and the surrounding electrons; therefore, in the present work we have carried out Mössbauer spectroscopy analysis so as to support our recently published results.

2. Experimental procedure

$Mg_{0.9}Mn_{0.1}Gd_yFe_{2-y}O_4$ nanoferrites, where $y=0.05$, 0.1, 0.2 and 0.3, have been prepared by the solution combustion technique. The chemical reagents used in the present work were ferric nitrate ($Fe(NO_3)_3\cdot 9H_2O$), gadolinium nitrate ($Gd(NO_3)_2\cdot 9H_2O$), magnesium nitrate ($Mg(NO_3)_2\cdot 6H_2O$) and manganese nitrate ($Mn(NO_3)_2\cdot 4H_2O$) and glycine (NH_2CH_2COOH) was used as a fuel. In a stoichiometric ratio all the above mentioned nitrates and glycine were dissolved in distilled water so as to obtain the precursor solution. The obtained precursor solution was then heated on a hot plate at 80 °C with a constant stirring till the solution starts to burn with liberation of lots of heat. The obtained powder

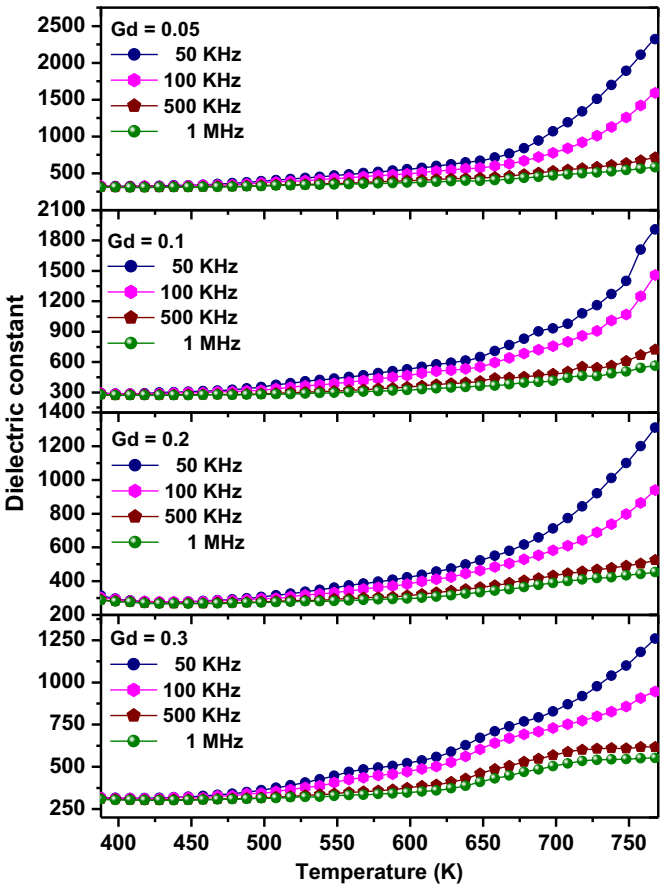

Fig. 2. Variation of dielectric constant with temperature at different frequencies for $Mg_{0.9}Mn_{0.1}Gd_yFe_{2-y}O_4$ nanoferrites.

samples were then calcined at 500 °C for 4 h. The calcined powders obtained for all the nanoferrites were then pressed into pellets of thickness 2 mm and diameter 10 mm under a pressure of 3–5 t/in^2. The prepared samples were then sintered at 700 °C for 4 h. The single-phase nature of the prepared samples was investigated by the X-ray diffraction (XRD) study which was carried out with Cu-K_α radiation of wavelength 1.54 Å using Rigaku-Denki X-ray diffractometer. The temperature dependence of dc resistivity of all the samples was studied with the help of Keithley instrument model 2611. The dielectric properties such as dielectric constant and dielectric loss have been investigated as a function of frequency in the range of 100 Hz to 1 MHz at different temperatures by using WAYNER KERR 6500 impedance analyzer. Mössbauer spectroscopy at room temperature was carried out by using a constant acceleration driven Mössbauer spectrometer model FAST Com Tec 070906. The experimental data is fitted with NORMOS (DIST) fitting package [22] and the best fit is considered for minimum deviation (χ^2) between experimental and theoretical spectrum.

3. Results and discussion

3.1. Structural study

The X-ray patterns of $Mg_{0.9}Mn_{0.1}Gd_yFe_{2-y}O_4$, $y=0.05$, 0.1, 0.2 and 0.3, nanoferrites, which indicated a typical cubic spinel structure were published by our group in our previous publication [21]. It has been reported by Shirsath et al. [23] that rare-earth doped ferrites show extra crystalline phases because of their low solubility and large ionic radii. The XRD patterns obtained for the

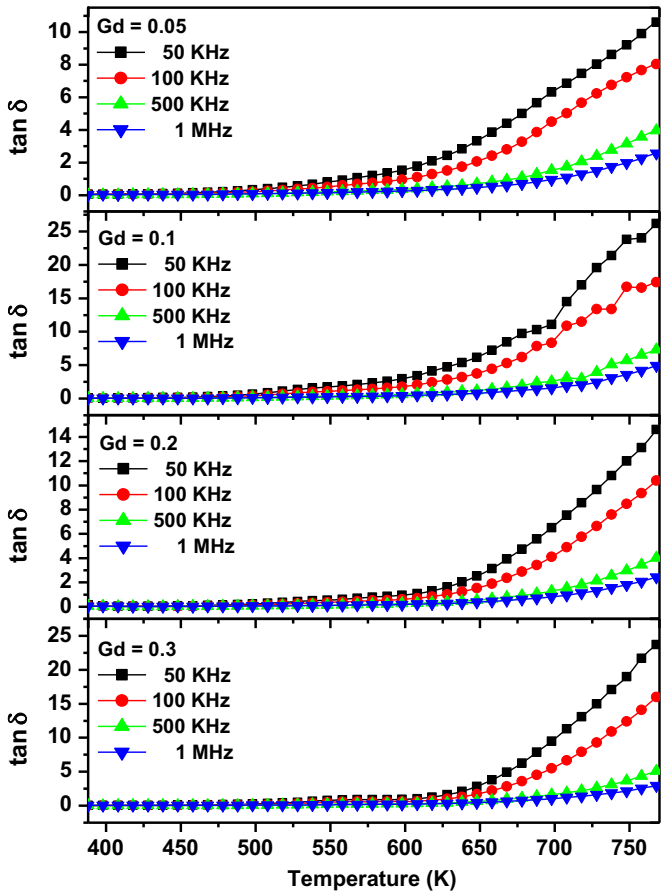

Fig. 3. Variation of dielectric loss with temperature at different frequencies for $Mg_{0.9}Mn_{0.1}Gd_yFe_{2-y}O_4$ nanoferrites.

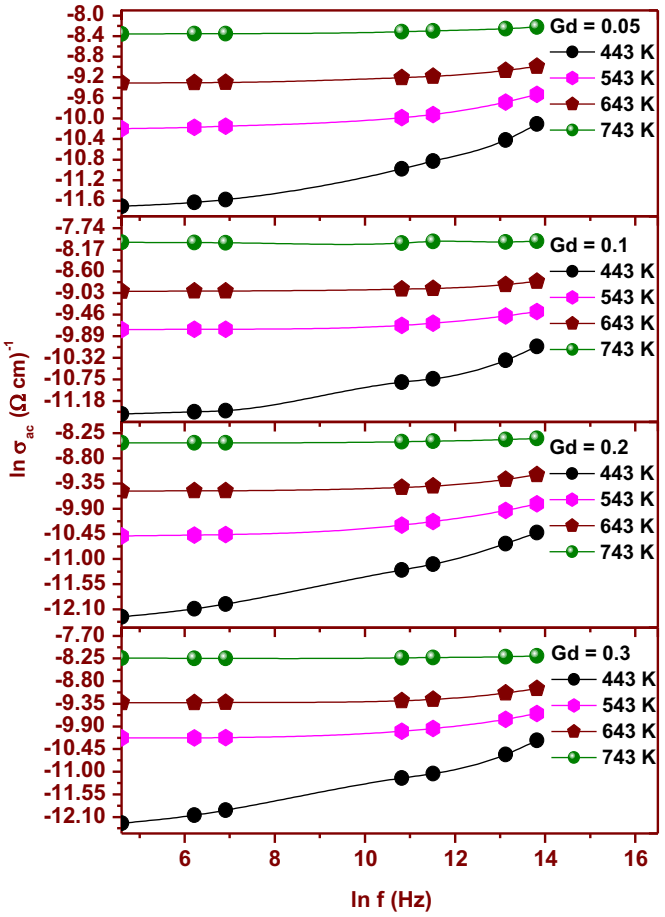

Fig. 4. Variation of ac conductivity with frequency at different temperatures for $Mg_{0.9}Mn_{0.1}Gd_yFe_{2-y}O_4$ nanoferrites.

present samples indicated that no unreacted constituents were present in the samples. The calculated values of particle size were observed to be 13.4 nm, 14.6 nm, 15.2 nm and 16.1 nm for $y=0.05$, 0.1, 0.2 and 0.3 respectively. The detailed structural analysis is presented by the author elsewhere [21].

3.2. Variation of dc resistivity with temperature

Fig. 1 shows the variation in dc resistivity as a function of temperature for all the synthesized nanoferrites. The dc resistivity is observed to be decreasing with an increase in temperature, i.e. exhibiting semiconducting behavior [24], according to the well known Arrhenius equation [25]:

$$\rho = \rho_0 \exp \frac{\Delta E}{kT} \tag{1}$$

where ΔE is activation energy, which is the energy needed to release an electron from the ion for a jump to the neighboring ion, thus giving rise to electrical conductivity, ρ_0 is pre-exponential factor, k is Boltzman constant, T is absolute temperature. The resistivity decrease with an increase in temperature because an increase in temperature will enhance the drift mobility of the charge carriers; since rise in temperature will help the bound charges to participate in the conduction process [26]. The calculated values of activation energy are given in Table 1. It is evident to Table 1 that ferrimagnetic region has lower activation energy values as compared to the paramagnetic region. The lower activation energy in the ferrimagnetic region is attributed to the magnetic disordering [27] due to the decrease in concentration of current carriers [28], while the change in activation energy is attributed to the change in conduction mechanism [29,30]. The change in activation energy for different compositions is attributed to the hoping of polarons. The values of activation energy above 0.2 eV clearly indicate the polaron hopping in the synthesized nanoferrites [31]. Further, from Fig. 2, it is evident that the dc resistivity is increasing with an increasing substitution of Gd^{3+} ions. In ferrites, the Fe^{3+} ions are moderately reduced to Fe^{2+} ions during sintering of ferrites, which results in the formation of a small amount of Fe^{2+} ions in these samples [32]. Also, a small fraction of Mn^{2+} ions reacts with Fe^{3+} ions to form Mn^{3+} and Fe^{2+} as per the following reaction:

$$Mn^{2+} + Fe^{3+} \rightarrow Mn^{3+} + Fe^{2+} \tag{2}$$

The presence of Fe^{2+}–Fe^{3+} and Mn^{2+}–Mn^{3+} ion pairs of the same element but of different valences present at the equivalent crystallographic sites are responsible for conduction due to hopping of electrons in $Mg_{0.9}Mn_{0.1}Fe_2O_4$ ferrites [33]. Since Gd^{3+} ions have a tendency to occupy octahedral sites, therefore, the addition of Gd^{3+} ions in Mg–Mn ferrites will directly reduce the number of B-site Fe^{3+} ions thus, limits the degree of conduction by blocking the Verwey's hopping mechanism [34] resulting an increase in resistivity.

3.3. Variation of dielectric constant with temperature

The value of dielectric constant was calculated by using the following relation [34]:

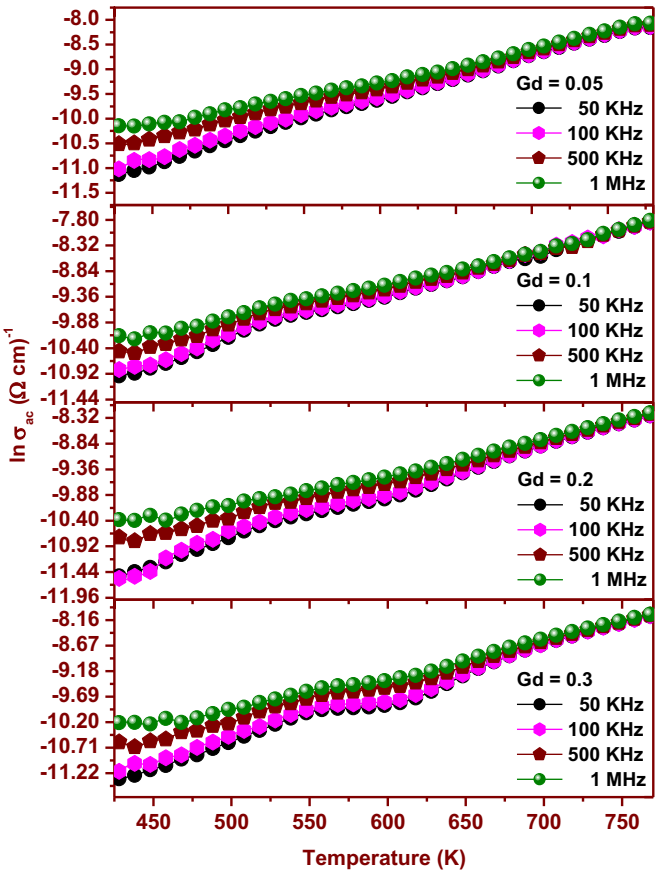

Fig. 5. Variation of ac conductivity with temperature at different frequencies for $Mg_{0.9}Mn_{0.1}Gd_yFe_{2-y}O_4$ nanoferrites.

$$\epsilon' = \frac{C_p\, d}{\epsilon_0\ A} \tag{3}$$

where ε_0 is the permittivity of free space, d is the thickness of the pellets, A is the area of cross-section of the pellets, and C_p is the measured value of the capacitance of the pellet. Fig. 2 shows the variations of dielectric constant (ε') as a function of temperature at different frequencies. Initially, the dielectric constant is observed to be increasing slowly with an increase in temperature while at higher temperature (beyond 650 K) a rapid increase in the dielectric constant is observed. Since the main contribution of dielectric constant is because of the different polarization mechanisms i.e. dipolar polarization, electronic polarization, ionic polarization and interfacial polarization, therefore, the observed behavior of dielectric constant (ε') can be explained on the basis of polarization effect. Interfacial polarization and dipolar polarization are well known to play the dominating role at low frequencies, and both of these polarizations are greatly affected by the temperature [26]. Interfacial polarizations generally originate due to the gathering of charges at the grain boundary. Since, the charge carriers in ferrites are not completely free but are strongly localized. When we increase the temperature, it is helping the bound charges to be free and is thermally activating their drift mobility too. This is amplifying the dielectric polarization due to which dielectric constant is observed to be increasing. Further, the results show that at all temperatures the dielectric constant is decreasing with an increase in frequency which is in accordance with the Maxwell–Wagner model [35,36]. According to this model, the dielectric structure is supposed to be composed of well conducting grains separated by the poorly conducting grain boundaries. The electronic exchange between Fe^{2+} and Fe^{3+} ions results in the local displacements of electrons along the direction of applied external field. These displacements are responsible for the polarization as well as the dielectric properties. The hopping mechanism is accountable to move the electrons towards the grain boundary. Generally, grain boundary has high resistance due to which electrons pile up there and create polarization [34]. When we increase the frequency then above certain frequency the electronic exchange between the ferrous and ferric ions does not follow the applied field resulting thereby decrease in the dielectric constant.

3.4. Variations of dielectric loss with temperature

Fig. 3 shows the variations of dielectric loss tangent ($\tan\delta$) as a function of temperature at different frequencies. It is evident from results that the dielectric loss tangent is increasing slowly with an increase in temperature while at higher temperature (beyond 650 K) it is increasing rapidly. As these variations are similar to dielectric constant therefore can be explained in a similar way. The energy losses in the dielectrics are because of the electric conductivity of the materials and the relaxation effect to the orientation of the dipole. The increase in the dielectric loss tangent with an increase in temperature is suggesting that with an increase in temperature, the losses due to dipole orientations are decreasing while the losses due to electric conductivity are increasing. Further, it is also evident from the results that at all temperatures the dielectric loss tangent is decreasing with the increase in frequency. These results are in close agreement with Koop's phenomenological model [37]. Generally, the dielectric loss come up when the polarization lags behind the applied altering field and is originate because of the existence of impurities and structural inhomogeneities. Thus, the low values of dielectric loss tangent achieved in the present work are therefore attributed to more structurally perfect and homogeneous nanoferrites synthesized by the solution combustion technique.

3.5. Variation of ac conductivity

The ac conductivity (σ_{ac}) is calculated from dielectric data using following relation [22]:

$$\sigma_{ac} = \varepsilon'\, \varepsilon_0\, \omega\ \tan\ \delta \tag{4}$$

where ε' is dielectric constant, ε_0 is permittivity of free space, $\tan\delta$ is loss tangent and ω is an angular frequency. Fig. 4 shows the variations of ac conductivity as a function of frequency at different temperatures. The plots for variations of ac electrical conductivity with frequency are observed to be almost linear confirming the polaron type conduction. The observed variation of ac conductivity as a function of frequency can be enlighten in view of Maxwell–Wagner heterogeneous model [35,36] of the polycrystalline structure of ferrites. In this model, the dielectric structure is divided into two layers. The first layer consists of well conducting ferrite grains which is separated by a second thin layer of weakly conducting substances termed as grain boundary. At lower frequencies these grain boundaries are more active due to which the hopping frequency of electron between Fe^{3+} and Fe^{2+} is less at lower frequencies. As the frequency of an applied field increases, the conductive grains become more active by encouraging the hopping of electron between Fe^{3+} and Fe^{2+} ions resulting thereby gradual increase in ac conductivity with frequency. Fig. 5 shows the variations of ac conductivity as a function of temperature at different frequencies. It is observed that the conductivity is increasing with the increase in temperature and is due to the thermally enhanced drift mobility of charge carriers. Further it is evident from the results that at high temperatures the

conductivity became almost frequency independent. This is because of the facts that at high temperature region the frequency independent part dominate; hence, the frequency dependence of ac conductivity becomes less significant.

3.6. Mössbauer spectroscopy analysis

Fig. 6 shows the room temperature Mössbauer spectra for $Mg_{0.9}Mn_{0.1}Gd_yFe_{2-y}O_4$ (y=0.05, 0.1, 0.2, 0.3) nanoferrites. The experimental data is fitted with NORMOS (DIST) program. The average values of hyperfine field and isomer shift are listed in Table 2. The isomer shift (IS) arises due to the electrostatic interaction between the charge distribution of the nucleus and those electrons that have a finite probability of being found in the region of the nucleus. Only s-electron wave functions have a finite value at the nucleus and these electrons are, therefore, responsible for this interaction. The isomer shift is a physical parameter for probing the valence state of a Mössbauer atom. It can be concluded from Table 2 that the observed value of average isomer shift is consistent with the presence of iron in 3^+ state. The splitting in the Mössbauer spectrum which originates because of the coupling between the nuclear magnetic moment and the magnetic field at the nucleus is called hyperfine interaction or Zeeman splitting. In general, the magnetic field can originate either within the atom itself, within the crystal via exchange interactions and from applied external field. The Hamiltonian for the interaction can be expressed as;

$$H_m = -\mu . H = -g\mu_N I . H \quad (5)$$

Table 2
Mössbauer parameters: average hyperfine field (HF), and average isomer shift (IS) of $Mg_{0.9}Mn_{0.1}Gd_yFe_{2-y}O_4$ nanoferrites.

y	HF field (T)	IS (mm/s)
0.05	39.20	0.58
0.1	33.95	0.50
0.2	31.60	0.52
0.3	30.84	0.524

$$H_m = -g\mu_N H I_Z \quad (6)$$

where μ_N is the nuclear Bohr magneton, μ is nuclear magnetic moment, I is the nuclear spin and g is the gyromagnetic ratio. The eigen values of Hamiltonian can be expressed as;

$$E_m = -g\mu_N H m_I \quad (7)$$

where m_I (m_I=+I, I-1, I-2,.....-I) is the magnetic quantum number representing the Z-component of I. The magnetic field therefore splits a nuclear spin I into $2I+1$ sublevels. A Mössbauer transition can take place if the change in the m_I value is 0 or ± 1. So in case of ^{57}Fe, the excited level I=3/2 splits into 4 sublevels and I=1/2 ground state splits into 2 sublevels, giving six Mössbauer transitions between these sublevels i.e sextet. The fluctuation of magnetization vectors in a direction close to an easy direction of magnetization leads to a particle size dependent magnetic hyperfine field. If the correlation time of the collective magnetization fluctuations is short relative to the observation time, the measured value of the magnetic field and consequently the hyperfine field will be reduced according to the equation:

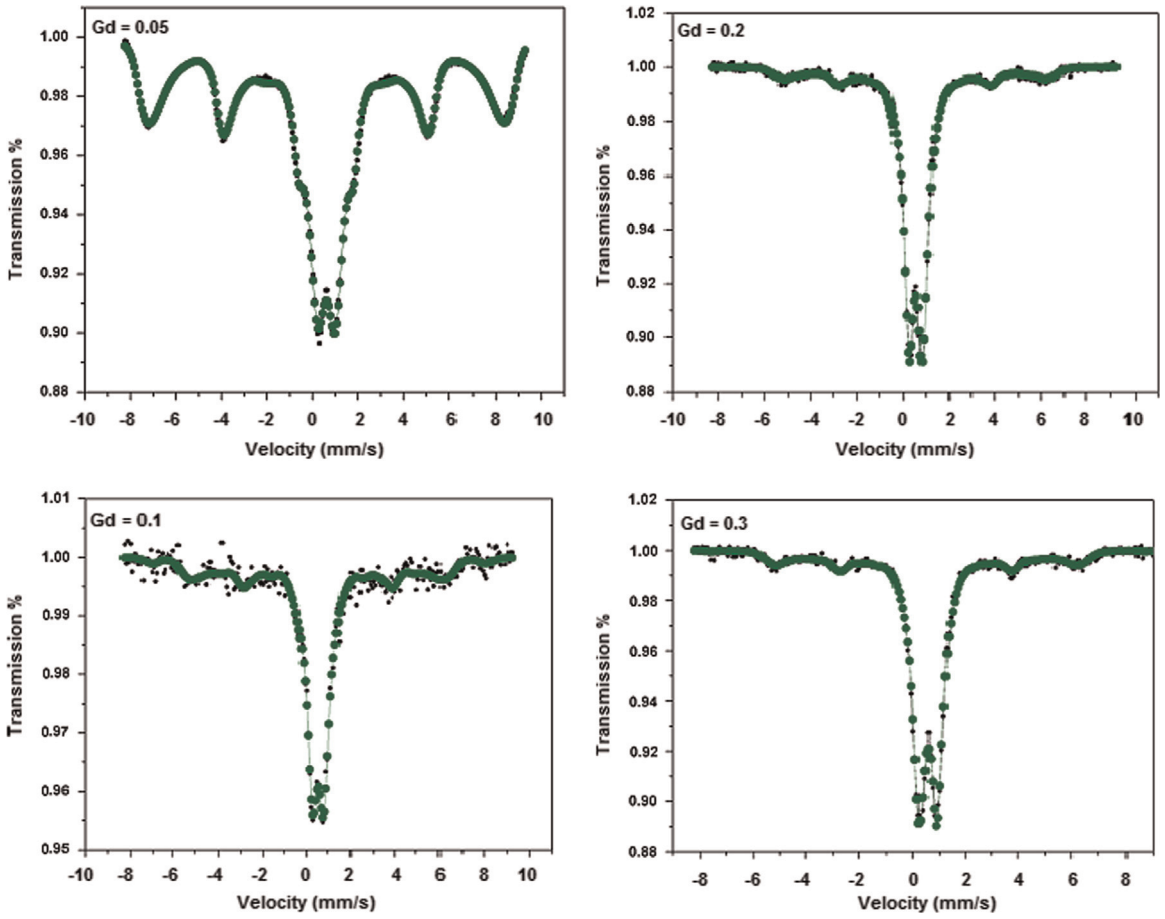

Fig. 6. Room temperature Mössbauer spectra for $Mg_{0.9}Mn_{0.1}Gd_yFe_{2-y}O_4$ nanoferrites.

$$H_{hf}(V, T) = H_{hf}(V = \infty, T)\left[1 - \frac{k_B T}{2KV}\right] \quad (8)$$

where k_B is the Boltzmann's constant, V is the particle volume and $V=\infty$, refers to a large crystals at temperature T in the absence of collective magnetic excitations. Therefore, according to Eq. (8) the hyperfine filed deceases with the decrease in particle size since particles with different volumes will show different hyperfine splitting. It can be seen from Fig. 6 that with the substitution of Gd^{3+} ions there are doublets in place of well defined sextets which indicates that incorporation of Gd^{3+} ions in the Mg–Mn nanoferrite matrix is making the system more non ferromagnetic. Further, it can be observed from Table 2 that average magnetic hyperfine field (HF) is decreasing with the increasing content of gadolinium ions in the Mg–Mn nanoferrite matrix inspite of the fact that particle size is increasing with the increasing substitution of Gd^{3+} ions. The observed variations in the magnetic hyperfine field show that the increasing content of gadolinium ions is weakening the A–B super-exchange interactions. Peng et al. [15] and Iqbal et al. [16] reported that the magnetic moments of the rare-earth ions usually originate from the localized 4f electrons; at room temperature, their magnetic dipolar orientation is disordered. In addition to this, Iqbal et al. [16] and Jing et al. [17] claimed that at room temperature, Gd^{3+} ions are non-magnetic ions having no contribution to the magnetization of doped ferrite. Since the magnetic moment of each composition depends on the magnetic moments of engaged ions, therefore, Neills et al. [18] also reported that magnetic moments of rare-earth ions are characterized by lower magnetic ordering temperatures, i.e lower than 40 K and their magnetic dipolar orientation is disordered at room temperature. So again they considered Gd^{3+} ions as non-magnetic ions, which make no contribution to the magnetization of doped ferrite at room temperature. Therefore, in view of the above reported papers [15–18,38–40], it can be concluded that apart from increasing trend of particle size, the non-magnetic contribution of the Gd^{3+} ions is resulting in doublets as well as is also responsible for the decreasing behavior of hyperfine field. The observed variations in the magnetic hyperfine field show that the increasing content of gadolinium ions is weakening the A–B super-exchange interactions and the same is in agreement with our recently published work [21].

4. Conclusions

Gadolinium substituted Mg–Mn nanoferrites were successfully processed by solution combustion technique. The dc resistivity is observed to be decreasing with an increase in temperature. Dielectric constant, loss tangent, and ac conductivity are observed to increase with an increase in temperature. Room temperature Mössbauer spectra of the synthesized nanoferrites showed an increase in the paramagnetic doublet with the increasing substitution of Gd^{3+} ions. The magnetic hyperfine field was observed to be decreasing with the increasing content of gadolinium ions. Therefore, suggesting that the increasing content of gadolinium ions is weakening the A–B exchange interactions. The very high values of dielectric constant and the low values of dielectric loss tangent are obtained in the present work which makes these nanoferrites very suitable for microwave applications.

Acknowledgments

One of the authors (Gagan Kumar) is thankful to Mr. Anurag Katiyar (National Physical Laboratory, New Delhi, India) for his constant support during this work. The authors K.M. Batoo and M. Shahbuddin would like to extend their sincere appreciation to the Deanship of Scientific Research at King Saud University for its funding through the Research Group Project no. RGP VPP-290.

References

[1] M. Hashim, Alimuddin, S. Kumar, S. Ali, B.H. Koo, H. Chung, Ravi Kumar, J. Alloy. Compd. 511 (2012) 107.
[2] P.S.A. Kumar, J.J. Shrotri, C.E. Deshpande, S.K. Date, J. Appl. Phys. 81 (1997) 4789.
[3] A.S. Albuquerque, J.D. Ardisson, W.A.A.A. Macedo, M.C.M. Alves, J. Appl. Phys. 87 (2000) 4352.
[4] S.T. Assar, H.F. Abosheiasha, M.K. Elnimr, J. Magn. Magn. Mater. 350 (2014) 12.
[5] A. Pradeep, P. Priyadharsini, G. Chandrasekaran, J. Magn. Magn. Mater. 320 (2008) 2774.
[6] P. Tartaj, M.P. Morales, S. Veintemillas-Verdaguer, T. Gonzalez-Carreno, C. J. Serna, J. Phys. D: Appl. Phys. 36 (2003) R182.
[7] C. Venkataraju, G. Sathishkumar, K. Sivakumar, J. Magn. Magn. Mater. 322 (2010) 230.
[8] Mahavir Singh, J. Magn. Magn. Mater. 299 (2006) 397.
[9] A. Lakshman, P.S.V. Subba Rao, K.H. Rao, Mod. Phys. Lett. B 24 (2010) 1657.
[10] Ravi Kumar, S.K. Sharma, Anjana Dogra, V.V. Shiva Kumar, S.N. Dolia, A. Gupta, M. Knobel, M. Singh, Hyperfine Interact. 160 (2005) 143.
[11] N. Okasha, J. Alloy. Compd. 490 (2010) 307.
[12] C.-Y. Tsay, S.-J. Liang, C.-M. Lei, Y.-C. Lin, C.-L. Lin, Ferroelectrics 435 (2012) 62.
[13] K.B. Modi, N.H. Vasoya, V.K. Lakhani, T.K. Pathak, J. Adv. Microsc. Res. 7 (2012) 40.
[14] T.K. Pathak, N.H. Vasoya, T.S. Natarajan, K.B. Modi, R.J. Tayade, Mater. Sci. Forum 764 (2013) 116.
[15] J. Peng, M. Hojamberdiev, Y. Xu, B. Cao, J. Wang, H. Wu, J. Magn. Magn. Mater. 323 (2011) 133.
[16] M. Asif Iqbal, et al., J. Alloy. Compd. 579 (2013) 181.
[17] J. Jing, Li Liangchao, Xu Feng, J. Rare Earths 25 (2007) 79.
[18] W.J. Nellis, S. Legvold, Phys. Rev. 180 (1969) 581.
[19] J. Chand, Gagan Kumar, P. Kumar, S.K. Sharma, M. Knobel, M. Singh, J. Alloy. Compd. 509 (2011) 9638.
[20] Balwinder Kaur, M. Arora, A. Shankar, A.K. Srivastava, Rajendra Prasad Pant, Adv. Mater. Lett. 3 (2012) 399.
[21] Gagan Kumar, Jyoti Shah, R.K. Kotnala, Virender Pratap Singh, Sarveena, Godawari Garg, Sagar E. Shirsath, Khalid M. Batoo, M. Singh, Mater. Res. Bull. 63 (2015) 216.
[22] R.A. Brand, J. Lauer, W. Keune, Phys. Rev. B 31 (1984) 1630.
[23] Sagar E. Shirsath, S.S. Jadhav, B.G. Toksha, S.M. Patange, K.M. Jadhav, J. Appl. Phys. 110 (2011) 013914.
[24] Gagan Kumar, Jagdish Chand, Anjana Dogra, R.K. Kotnala, M. Singh, J. Phys. Chem. Solids 71 (2010) 375.
[25] S.E. Shirsath, B.G. Toksha, M.L. Mane, V.N. Dhage, D.R. Shengule, K.M. Jadhav, Powder Technol. 212 (2011) 218.
[26] J. Chand, Gagan Kumar, P. Kumar, S.K. Sharma, M. Knobel, M. Singh, J. Alloy. Compd. 509 (2011) 9638.
[27] K. Barerner, P. Mandal, R.V. Helmolt, Phys. Status Solidi B 223 (2001) 811.
[28] J. Baszsynski, Acta Phys. Polym. 35 (1969) 631.
[29] V.R.K. Murthy, J. Sobhandri, Phys. Status Solidi A 38 (1977) 647.
[30] R.B. Pujar, S.N. Kulakarni, B.K. Chougule, Mater. Sci. Lett. 15 (1996) 1605.
[31] S. Mishra, K. Kundu, K.C. Barick, D. Bahadur, D. Chakravorty, J. Magn. Magn. Mater. 307 (2006) 222.
[32] J.B. Goodenough, A.L. Loeb, Phys. Rev. 98 (1955) 391.
[33] M. Singh, S.P. Sud, Mod. Phys. Lett. B 14 (2000) 531.
[34] Gagan Kumar, Jyoti Shah, R.K. Kotnala, Pooja Dhiman, Ritu Rani, Virender Pratap Singh, Godawari Garg, Sagar E. Shirsath, Khalid M. Batoo, M. Singh, Ceram. Int. 40 (2014) 14509.
[35] K.W. Wagner, Ann. Phys. 40 (1913) 817.
[36] J.C. Maxwell, Electricity and Magnetism, Oxford University Press, Oxford, 1973.
[37] C.G. Koops, Phys. Rev. 83 (1951) 121.
[38] E. Pervaiz, I.H. Gul, Int. J. Curr. Eng. Technol. 2 (2012) 377.
[39] J.L. Bhosale, S.N. Kulkarni, R.B. Sasmile, B.K. Chougule, Bull. Mater. Sci. 19 (1996) 767.
[40] R. Islam, M.A. Hakim, M.O. Rahman, H.N. Das, M.A. Mamun, J. Alloy. Compd. 559 (2013) 174.